

# **Comparison of measurement procedures for evaluating thermal errors of machine tools due to moving linear axes**

Michael L. McGlaufflin, Johannes A. Soons, M. Alkan Donmez

*National Institute of Standards and Technology, USA*

## **Abstract**

This paper investigates an alternative method to assess thermal errors due to the heat generated by moving linear axes. This method is based on a spindle-mounted probe and simple artifacts. The angular errors introduced by the heating of individual axes (X, Y, and Z) are obtained by probing multiple points on table-mounted artifacts. A discussion is presented of how the errors of the axes are estimated from changes in the location of points on artifacts. Repeatability testing and comparison with data taken by an independent laser-based system verify the performance. The paper describes the design of the test, sign conventions, and analysis procedure. The results show excellent repeatability and good correlation to data gathered with the laser-based system.

## **Introduction**

Thermal errors are a key impediment to precision in machining. Machine tool structures are subject to deformations due to temperature gradients caused by: 1) non-uniform heating of the work-piece and machine structural components and/or 2) uniform heating of nonsymmetrical structures. International and U.S. national standards on machine tool performance contain parameters and procedures that enable users to specify and verify the sensitivity of machine accuracy to key heat sources.

The ISO 230-3 standard, "Determination of thermal effects" [1], addresses the thermal errors caused by linear axis motions through the determination of the drift in the positioning errors of an axis after exercising the axis through high-speed back-and-forth motions. In other words, only errors in the direction of axis

motion (position error) are assessed. For machine tools that rely on the lead screw for position feedback instead of an independent scale, these errors can be major due to the significant temperature rise of lead screws that are not cooled [2]. Currently there is an effort to revise the ISO standard to introduce additional tests and parameters to evaluate the thermal drift in the angular and straightness errors of each axis [3]. Such errors can be introduced through changes in preloads and warping of the guide-ways as a result of thermal gradients [4].

The U.S. national standard, ANSI/ASME B5.54, "Performance evaluation of computer numerically controlled machining centers" [5], has essentially the same test and performance parameters as ISO 230-3. The differences between the two standards are found mainly in the quantitative elements of each test description. The ASME standard, however, includes an easy-to-perform test for thermal drifts in the position and orientation of the tool due to high-speed axis motions. The drifts are measured at one point in the machine work-volume using a five-probe nest and spindle-mounted artifact. After each measurement, all axes are exercised and the artifact is returned to the nest for the next measurement.

In this study we evaluate the application of a spindle-mounted probe to assess thermal drifts in all the parametric errors of a linear-axis due to the heat generated by the axis.

### **Description of the tested machine and sign convention**

The machine tool used in this research was a vertical five-axis high-speed-machining center with an integrated touch-trigger probe (Figure 1).

The machine is comprised of stacked slides (Z on Y on X) that move the tool and separately stacked rotary axes (C on B) that move the work-piece. Linear glass scales provide positioning feedback for the linear axes.

Sign conventions for this research reflect motion of the tool relative to the work-piece and are defined with the machine coordinate system (Figure 1).

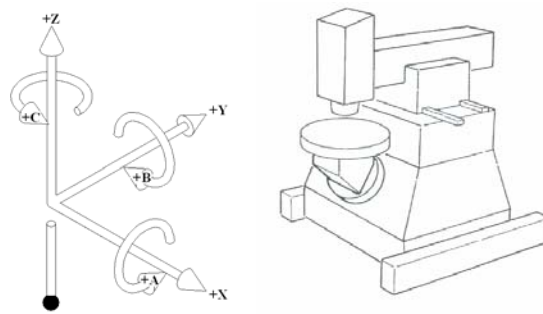


Figure 1: Machine-tool structure and sign convention

## Comparison of measurement methods

Various techniques have been proposed to measure the thermal drifts of the three displacement and three angular errors of a linear machine tool axis. They can be grouped into three classes:

- 1) Application of conventional artifacts and instruments designed for the measurement of geometric axis errors. (e.g., laser interferometer and straight edge)
- 2) Application of a nest of displacement probes (sensor nest) mounted on the table [5] or spindle [1]. Changes in the readings of the probes can be used to calculate drifts in the orientation and position of the tool relative to the work-piece.
- 3) Application of a spindle probe to measure changes in the location of points on artifact(s) mounted on the work table, the results of which can be used to estimate changes in the relative position and orientation of the spindle [3]. This approach is new and is the focus of this study.

Class 1 tests require additional equipment, care in the setup, and are time-consuming. The reference is fixed and many points within the work volume can be measured.

Class 2 tests can require machine axes motions other than the test axis. In general only a few points are assessed and for large machines the table is often part of the reference.

Class 3 tests are similar to Class 2, but are easier to execute as they do not require additional instrumentation. Depending on the configuration of artifact and probe, assessed angular errors may be only part of the structural loop.

The sensor-nest and probe methods yield similar results for errors in the relative position of the spindle and work component. For angular errors, the methods yield different results. The sensor-nest method obtains the angular drift due to deformation of the entire structural loop. The probe method only yields the angular errors in that part of the structural loop where the Abbe offset changes when measuring multiple points on the artifact. Two mechanisms are available to change the Abbe offset: 1) use of a Star-probe or 2) displacement of a machine axis. If a Star-probe is not used, the estimated angular errors do not address the complete structural loop. In this study we focus on this case as it reflects the common configuration of machine-tool probing systems.

An angular error is estimated by the observed difference in the errors of two points divided by the respective change in Abbe offset. Which points are probed and the direction in which they are probed determines the data's sensitivity to angular errors. For example, Figures 2a and 2b are simplified views of the test machine structure with an exaggerated rotation of the Z-axis through the YZ plane. The probing motion is in the  $-Z$  direction and the change in the Abbe offset is in the Y-axis. As a result, this probing cycle is insensitive to any angular error in the Z-axis because there is no change in the Z-axis Abbe offset. A drift in the roll of the X-axis does see a change in Abbe offset and will be obtained.

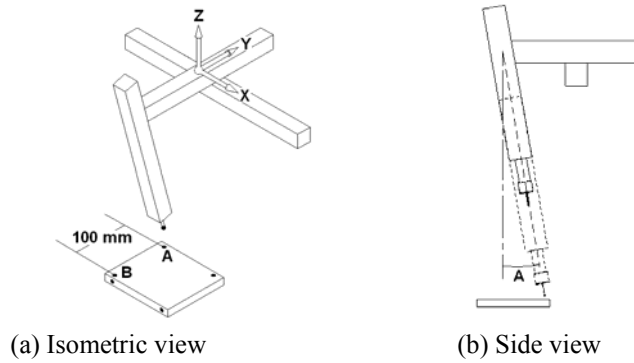


Figure 2: Insensitivity to particular errors

An examination of artifact designs and probing points, and its impact on the relevance of the resultant data follows. Evaluation of X-axis errors can be carried out using probing points listed in Table 1 for the artifact configurations given in Figure 3.

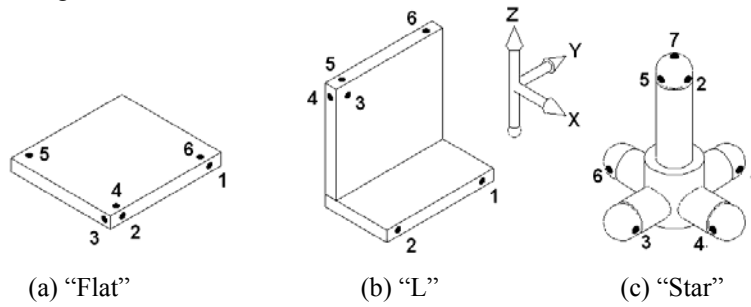


Figure 3: Artifacts and probed points for a thermal test of the X-axis

Table 1: Evaluation of X-axis probing points

Error	Flat	L	Star
$\Delta X$	2	2	2
$\Delta Y$	3	4	5
$\Delta Z$	4, 5 or 6	5 or 6	7
$\Delta A$	6-4**	6-5**	$((4+6)/2)-5^*$
$\Delta B$	5-4***	3-2*	$2-((1+3)/2)^*$
$\Delta C$	2-1**	2-1**	3-1**

- \* Excludes the structural loop between Z slide and probe
- \*\* Excludes the structural loop between Y slide and probe
- \*\*\* Excludes the structural loop between X slide and probe

Artifact design can be adjusted to focus on an area of interest. The Star design addresses a large part of the structural loop because of its more extensive use of Z-axis motions to generate differences in Abbe offset. Even with this design however the complete structural loop is not addressed. For example, an angular drift in spindle-probe interface cannot be assessed.

Referring to Figures 4a, 4b and 4c, the Y, and Z-axes present a similar view of the analysis, as presented in Tables 2 and 3.

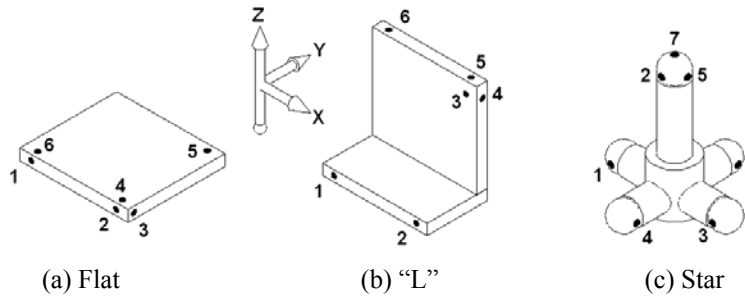


Figure 4: Artifacts and probed points for thermal tests of the Y and Z-axes

Table 2: Evaluation of Y-axis probing points

Error	Flat	L	Star
$\Delta X$	3	4	5
$\Delta Y$	2	3	2
$\Delta Z$	4	5	7
$\Delta A$	5-4**	2-3*	$((1+3)/2)-2^*$
$\Delta B$	6-4***	6-5***	$5-((4+6)/2)^*$
$\Delta C$	2-1***	2-1**	4-6**

Table 3: Evaluation of Z-axis probing points

Error	Flat	L	Star
$\Delta X$	3	4	5
$\Delta Y$	2	3	2
$\Delta Z$	4	5	7
$\Delta A$	5-4**	3-2*	$((4+5)/2)-6^*$
$\Delta B$	6-4***	6-5***	$3-((1+2)/2)^*$
$\Delta C$	2-1***	2-1***	4-6***

- \* Excludes the structural loop between Z slide and probe
- \*\* Excludes the structural loop between Y slide and probe
- \*\*\* Excludes the structural loop between X slide and probe

## Measurement setup and test procedures

The two artifacts used in this research were the “Flat” and “Star” designs in Figures 3a and 3c. For the X, and Y-axis tests, the measurement positions for each test series is 150 mm on either side of the C-axis center of rotation.

For Z-axis measurements one artifact was positioned on the table and the other on a 300 mm riser block. A Y-axis offset of 120 mm between the artifacts was required to avoid collision of the upper artifact and spindle.

The minimum resolution of the probed coordinates (.001 mm) and the distance between point pairs (100 mm) limits the angular resolution to 2 arc seconds.

The machine was programmed to probe each artifact, and then exercise the axis back and forth for 10 min at 7000 mm/min. This was repeated 24 times resulting in a 4 h duty cycle.

Fifteen thermocouple temperature sensors were used to monitor machine structural components and the environment.

Verification measurements were performed using a commercially available laser-based system capable of measuring all parametric errors simultaneously. The machine and data capture were programmed to imitate the artifact data gathering process such that the heat input was similar.

## Test Results

The following graphs compare drift measurements in angular errors when exercising individual linear axes as measured with Flat and Star artifacts and a laser-based system. These are representative samples of data gathered at the two measurement positions previously described. All laser-based position and transversal results were Abbe Error corrected to spindle gage-line.

Ambient temperatures for each test are omitted for reasons of clarity. The maximum ambient temperature change during a four hour test was 2.0 °C.

Figures 5, 6, and 7 show data gathered during Y-axis evaluation tests. Figure 5 shows an excellent agreement between the Star artifact and laser.

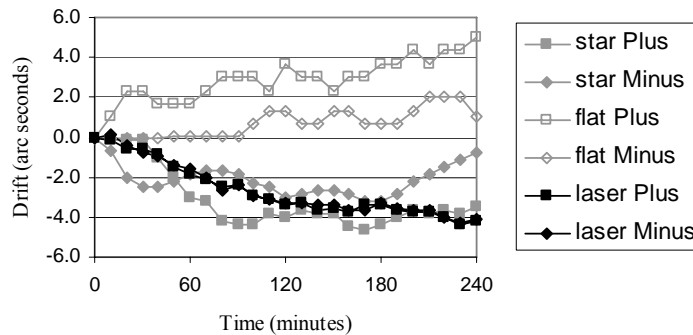


Figure 5: Comparison of angle B during a Y-axis test (EBY)

Figure 6 is an example of an excellent agreement between the experimental results of the Star artifact and laser-based system. As indicated in Table 3, the Flat artifact addresses a significantly smaller part of the machine structure which explains the lack of correlation.

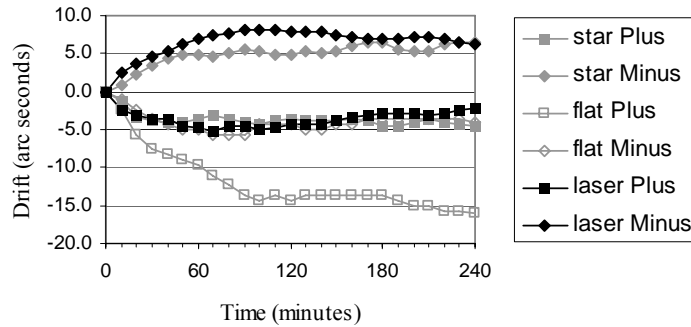


Figure 6: Comparison of angle A during a Y-axis test (EAY)

When angular error results are used to correct position data, the measurement discrepancy is further magnified. Figure 7 shows Y-axis position data Abbe error corrected to the spindle gage-line. At the, “Minus” position the Y-axis is extended away from its support structure, which results in a larger pitch error than that at the, “Plus” position and consequently a larger disagreement in the position data.

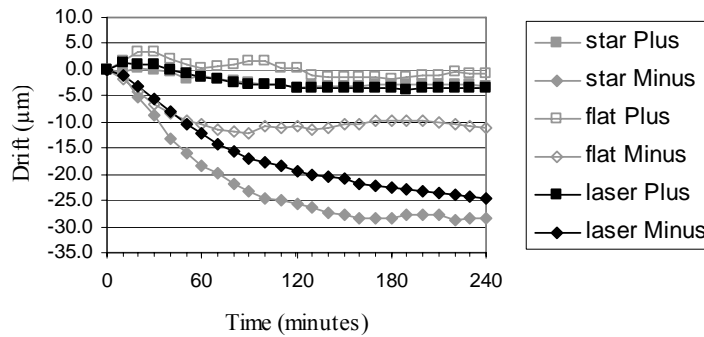


Figure 7: Evaluation of corrected position data during a Y-axis test (EYY)

As expected from the evaluation analysis there is little difference between the two artifact designs when evaluating a rotation around the Z-axis (Figure 8). Both artifact designs utilize the same displacement of the Y-axis.

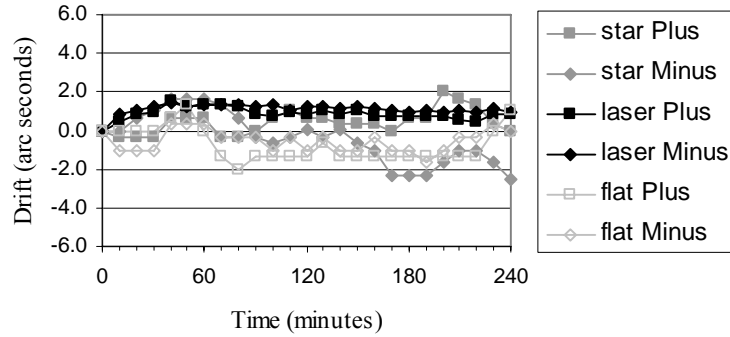


Figure 8: Comparison of angle C during a Y-axis test (ECY)

### Uncertainty Analysis

The comparison could only be executed through sequential experiments. Therefore the comparison relies on the assumption that the machine warm-up behavior is repeatable. Several experiments were executed to validate this assumption; a typical result is shown in Figures 9 and 10. The uncertainty analysis of the two measurement methods does not include uncertainty in the thermal expansion of the machine.

The uncertainty of thermal drift obtained using the artifact is determined by the thermal stability of the artifact and probe and the probing repeatability. The probing repeatability was determined by ten repeated measurements in X, Y, and Z. The respective expanded uncertainty  $U_p$  ( $k=2$ ) is shown in table 4. The resulting uncertainty  $U_a$  in an estimated angle for an Abbe offset of 100 mm is calculated as follows:

$$U_a^2 = 2U_p^2 / 100^2$$

Table 4: Uncertainty analysis

Device	Positioning	Straightness	Angular
Machine & Probe Repeatability	.002 mm	.002 mm	2.8 arc sec
Probe thermal expansion (in Z)	.008 mm	.008 mm	

Laser repeatability (Figure 9) and stability (Figure 10) tests were run over 3 consecutive days. Position, straightness, and angular uncertainty were calculated as above. Results are given in table 5. The expanded uncertainty is  $U = .0119$  mm ( $k=2$ ) [6].

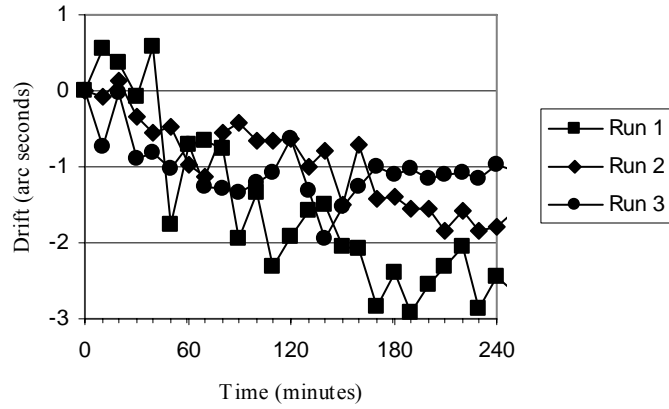


Figure 9: Machine and laser repeatability tests (angle B)

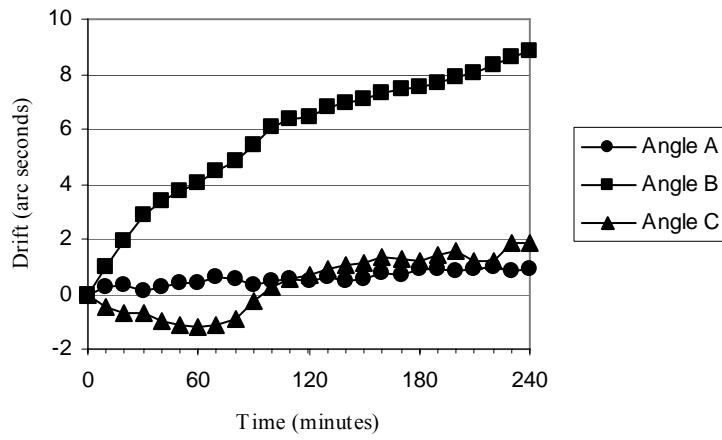


Figure 10: Results of a laser stability test

Table 5: Machine and laser expanded uncertainty (k=2)

Device	Position	Straightness	Angular
Machine & Laser Repeatability	.0018 mm	.0018 mm	.04 arc sec

## Conclusions

Artifact-based performance evaluation is practical. It shows potential as an alternative to traditional methods when the artifact design is based upon the structure of the machine tool under test. It also offers the opportunity for reversal measurements that other artifact designs do not. For angular errors, only part of the structural loop is addressed when using a straight probe tip. In a few cases further investigation is needed where expected and experimental agreement was lacking.

This methodology may prove most useful for multi-axes or composite testing. Laser-based systems require multiple setups or, for those systems capable of evaluating more than one degree of freedom at a time, complicated and time-consuming alignment and evaluation. The artifact method does not require instruments or complex alignments and provides flexibility in the number and location of points where drifts are measured. Artifact probing also has the potential for integration into smart machining systems for self-evaluation.

This Publication was prepared by a United States Government employee as part of official duties and is, therefore, a work of the U.S. Government and not subject to copyright.

## References

1. ISO 230-3, Test code for machine tools - Part 3: Determination of thermal effects, 2001
2. Braasch, J., Position Measurement on Machine Tools: by Linear Encoder or Ballscrew and Rotary Encoder?, <http://www.heidenhain.com/posmeas.html>, 2004
3. ISO/CD 230-3, Test code for machine tools - Part 3: Determination of thermal effects, 2003
4. Beltrami, O., A deeper investigation into the thermal drift of a linear axis, Laser Metrology and Machine Performance IV, Proceedings of the 4<sup>th</sup> International Conference on Laser Metrology and Machine Performance – Lamdamap, 1999, pp. 357-367
5. ASME/ANSI B5.54, Methods for Performance Evaluation of Computer Numerically Controlled Machining Centers, 2005
6. NIST TN1297, Guidelines for Evaluating and Expressing the Uncertainty of NIST Measurement Results, 1994